THE ASTROPHYSICAL JOURNAL, 501:L221–L225, 1998 July 10

THE ROTATION PERIOD OF C/1995 O1 (HALE-BOPP)

JAVIER LICANDRO,[1,2] LUIS R. BELLOT RUBIO,[1] HERMANN BOEHNHARDT,[3] RICARD CASAS,[1] BENEDIKT GÖETZ,[4] ANGEL GÓMEZ,[1] LAURENT JORDA,[5] MARK R. KIDGER,[1] DAVID OSIP,[6] NANCI SABALISCK,[1] PABLO SANTOS,[1] MIQUEL SERRA-RICART,[1] GIAN PAOLO TOZZI,[7] AND RICHARD WEST[8]

Received 1998 February 25; accepted 1998 May 12; published 1998 June 26

ABSTRACT

C/1995 O1 (Hale-Bopp) was observed in daylight on 16 days between 1997 April 1 and 1997 April 28, five of which had long time sequences (up to 10 hr of data), using the near infrared CAIN camera on the 1.5 m Carlos Sánchez Telescope at Teide Observatory (Tenerife, Canary Islands, Spain). Three spiral dust jet structures were observed for several almost complete rotations. A nucleus rotation period of 11.34 ± 0.02 hr was determined from two different methods. No variations of the rotation period with time due to precessional effects were found in our data. However, the time sampling of the observations, similar to the suggested spin precession period, prevents us from ascertaining whether such variations exist. We note, though, that the good agreement of our results with the rotation periods at different epochs reported by other groups suggests that if they exist, these variations must be small, hence the rotation cannot be very complex.

Subject heading: comets: individual (Hale-Bopp 1995 O1)

1. INTRODUCTION

Dust and gas jets have been observed since the last century in the comae of bright comets. The most simple explanation for them is the presence of active areas on the surface of the rotating nucleus. For some favorable cases, modeling of jet structures observed in the coma permits to search for the rotational parameters of the nucleus (e.g., Sekanina 1981).

C/1995 O1 (Hale-Bopp) (hereafter Hale-Bopp) is an exceptionally active comet. The early detection of spiral jets during 1995 (Kidger et al. 1996) encouraged us to run a long-term observational campaign using the facilities available at Teide Observatory (Instituto de Astrofísica de Canarias). The main goal of this campaign was the observation of jet structures in order to derive the rotational parameters of the comet.

In this Letter, we present the observations carried out by the Hale-Bopp European Team using the Carlos Sánchez Telescope at Teide Observatory in 1997 April. From these observations we study the rotation period of Hale-Bopp's nucleus.

2. OBSERVATIONS

Hale-Bopp was observed on a total of 16 days with the Carlos Sánchez Telescope from 1997 April 1 to April 28. On five of these days, the comet was observed for several hours (up to 10). For the analysis presented here, we use the data summarized in Table 1, which correspond to the days with the longest data strings.

2.1. *Observing Procedure*

Near-infrared images of Hale-Bopp were obtained during daytime, from 1997 April 1 to April 28, with the 1.5 m Carlos Sánchez Telescope at Teide Observatory, using CAIN, the 1–2.5 μm camera. CAIN uses a NICMOS detector (256 × 256, 40 μm square pixels). The plate scale was $0\farcs39$ pixel^{-1}. Narrowband Brγ (2.166 μm), CO (2.295 μm), and $K_{\rm con}$ (2.26 μm) filters were used.

Since the observations were mainly performed during daytime, the shortest exposure time allowed by CAIN (0.4 s for a whole frame image) was used to avoid sky background saturation. Groups of 20–50 images were taken, producing total exposure times between 8 and 20 s. Sky images were obtained at distances between $5'$ and $10'$ from the central condensation and in the four cardinal directions. Series of 30 × 0.4 s images in each filter were taken in the following sequence: comet, sky $5'$ north, comet, sky $5'$ south, comet, sky $5'$ east, comet, and sky $5'$ west.

2.2. *Reduction Procedure*

Images were bias corrected using daily bias frames. Additionally, flat fielding was applied. Flat-field images were obtained by combining all of the available sky frames to give a high signal-to-noise ratio (S/N) master sky flat for each day of observation. For each group of images, all of the frames were co-added to produce a single master frame. Finally, all of the master frames in the same filter within 10 minute intervals were recentered, combined to produce the highest S/N frame possible without destroying the temporal evolution of the coma structures, and scaled to the same pixel size in kilometers at the comet's geocentric distance. Images of poor quality or having a discrepant centroid (due, for instance, to hot pixels or poor guiding) were excluded.

Observing conditions were generally difficult due to the presence of the Sun above the horizon and very close to the comet (~30°). Very fast sky level variations and direct solar light inside the dome complicated both the observations and the data

[1] Instituto de Astrofísica de Canarias, c/Vía Láctea, s/n, E-38200 La Laguna, Tenerife, Spain; jlicandr@ll.iac.es, lbellot@ll.iac.es, rcr@ot.iac.es, agomez@ot.iac.es, mrk@ll.iac.es, nss@ll.iac.es, psantos@ll.iac.es, mserra@ot.iac.es.

[2] Departamento de Astronomía, Facultad de Ciencias, Universidad de la República Oriental del Uruguay, and Observatorio Astronómico Los Molinos, Tristán Narvaja 1674, 11.200-Montevideo, Uruguay.

[3] European Southern Observatory, Santiago de Chile, Chile.

[4] University of München, Scheinerstrasse 1, D-81679 München, Germany; hboehnha@sc.eso.org.

[5] Max Planck Institute für Aeronomie, Max-Planck-Strasse 2, D-37191 Katlenburg-Lindau, Germany; jorda@linax1.mpae.gwdg.de.

[6] University of Florida, 211 Bryant Space Science Center, Gainesville, FL 32611-2055; osip@astro.ufl.ed.

[7] Osservatorio Astrofisico di Arcetri, Largo Enrico Fermi 5, 50125 Firenze, Italy; tozzi@arcetri.astro.it.

[8] European Southern Observatory, Karl-Schwarzchild-Strasse 2, D-85748 Garching, Germany; rwest@eso.org.

TABLE 1

SUMMARY OF THE DATA USED IN THIS LETTER

Date (1997 April) (1)	UT Start (2)	UT End (3)	Hours (4)	Images (5)	Weather (6)
1	9:27	19:39	10:12	40	PP
2	9:06	10:10	1:04	9	NP
7	13:29	19:24	5:55	38	P
8	19:27	19:38	0:11	4	NP
9	10:17	19:19	9:02	52	P
16	19:24	20:13	0:49	5	NP
18	18:10	20:04	1:56	9	NP
25	14:30	18:59	4:29	25	PP
27	11:18	20:05	8:47	56	P
28	12:05	20:02	7:57	36	PP

NOTE.—Cols. (2) and (3): UT of the first and last Hale-Bopp image obtained that day; col. (4): interval covered; col. (5): number of final images as explained in § 2; col. (6): observing conditions for each day—P = photometric, PP = partially photometric, and NP = nonphotometric.

reduction, causing many images to be discarded before the final image combination.

3. OBSERVED FEATURES

In order to enhance the structures observed in the coma, we applied a Laplacian filtering technique to the final images, as described in Kidger et al. (1998). The results for a set of selected images are presented in Figure 1; a log of these images is presented in Table 2. Images are ordered day by day, according to the rotational phase (computed as the fractional part of the time in hours since 1997 April 1.0 UT, divided by 11.35, i.e., the period determined later in this Letter). Several dust spiral jets and shells are observed. Dots and lines are the result of cosmetic defects of the camera (hot pixels) and the recentering procedure applied to the raw images.

After a careful inspection, we find that the appearance of the coma structures is identical in the images obtained with all three filters. Since there is no gas emission known to appear in comets in the K_{con} band, we used the K_{con} images to substract the continuum from some CO images. No prominent features due to CO emission are observed. We therefore attribute the coma structures to dust jets rather than to gas emission.

At least three different dust spiral jets (labeled A, B, and C), rotating counterclockwise, can be observed in Figure 1. Great care has to be taken in the identification of the jets, since in some rotational phases they appear superposed due to projection effects. At phase 0.0, A is the sole jet emerging from the nucleus (see, e.g., image 1-0.0, where 1 corresponds to the day column and 0.0 to the rotational phase in Fig. 1, as labeled in Table 2). Another curved jet (B) appears at phase 0.2 (images 7-0.2, 9-0.2). At phase 0.3 (image 7-0.3), jet A seems to be disconnected from the nucleus. The shell produced by A expands in the following phases, while jet B grows and rotates. At phase 0.7 (image 1-0.7) jet A appears again, whereas at phase 0.9 (image 7-0.9) jet B seems to be disconnected from the nucleus producing another shell structure. Notice that in the second half of April, jet B is clearly a double structure (jets B and C in images 25-0.7, 27-0.7, and 28-0.8). It could be possible that jets B and C were produced by two different nearby active regions. At the beginning of April, they appeared superposed because of the comet-Sun-Earth geometry, but in the second half of April the varying geometry made it possible to separate them.

The counterclockwise rotation of the jets and their curved shape indicate that the north pole of the nucleus was oriented to the Earth in 1997 April. This is in good agreement with the pole position reported by Licandro et al. (1998) (R.A. = 275°, decl. = −50°), Jorda et al. (1998) (R.A. = 275°, decl. = −57°), and Sekanina (1998) (R.A. = 257°, decl. = −61°). Given these orientations, the aspect angle (defined as the angle subtended by the comet spin axis to the line of sight) did not change much in April. For the first pole position, the comet aspect angle varied from 45° to 31° and the position angle of the spin axis varied from 237° to 213° during 1997 April.

TABLE 2

OBSERVING LOG FOR THE IMAGES USED IN FIGURE 1

Image	Date (UT April)	Phase	Filter
1-0.0	1.491	0.038	K_{con}
1-0.2	1.587	0.242	CO
1-0.6	1.774	0.637	CO
1-0.7	1.818	0.730	CO
1-0.8	1.394	0.917	CO
1-0.9	1.463	0.980	CO
7-0.0	7.626	0.012	CO
7-0.1	7.688	0.141	CO
7-0.2	7.735	0.244	CO
7-0.3	7.789	0.356	CO
7-0.4	7.806	0.391	CO
7-0.5	8.818	0.532	CO
7-0.8	7.562	0.876	Brγ
7-0.9	7.598	0.952	CO
9-0.0	9.547	0.072	K_{con}
9-0.1	9.606	0.197	CO
9-0.2	9.633	0.256	K_{con}
9-0.3	9.708	0.415	K_{con}
9-0.5	9.793	0.594	CO
9-0.6	9.805	0.619	K_{con}
9-0.8	9.429	0.824	Brγ
9-0.9	9.486	0.944	Brγ
25-0.1	25.604	0.142	K_{con}
25-0.4	25.750	0.451	K_{con}
25-0.5	25.791	0.537	K_{con}
25-0.7	18.800	0.704	CO
27-0.1	27.559	0.161	K_{con}
27-0.2	27.602	0.252	CO
27-0.3	27.629	0.309	K_{con}
27-0.5	27.744	0.553	K_{con}
27-0.6	27.797	0.663	K_{con}
27-0.7	27.837	0.748	K_{con}
27-0.9	27.477	0.988	K_{con}
28-0.1	28.503	0.158	CO
28-0.2	28.565	0.287	CO
28-0.3	28.612	0.388	CO
28-0.4	28.626	0.417	Brγ
28-0.6	28.749	0.677	CO
28-0.7	28.796	0.776	K_{con}
28-0.8	28.817	0.822	K_{con}

NOTE.—Phase is the rotational phase computed for the 11.35 hr rotation period.

4. DETERMINATION OF THE ROTATION PERIOD

On April 1 we have a 10 hr data string (with a gap of 3 hr during which no observations could be performed). As expected from the rotation period of ~11 hr reported by Jorda et al. (1997) and Sarmecanic et al. (1997), similar structures are observed in the images obtained at the beginning and the end of this day (compare, e.g., image 1-0.8 taken at 9:27 UT and 1-0.7 taken at 19:38 UT in Fig. 1).

We have computed the rotational phase of each image, as defined in § 3, but for a series of different rotation period values. For each rotation period, we visually compared all of the images

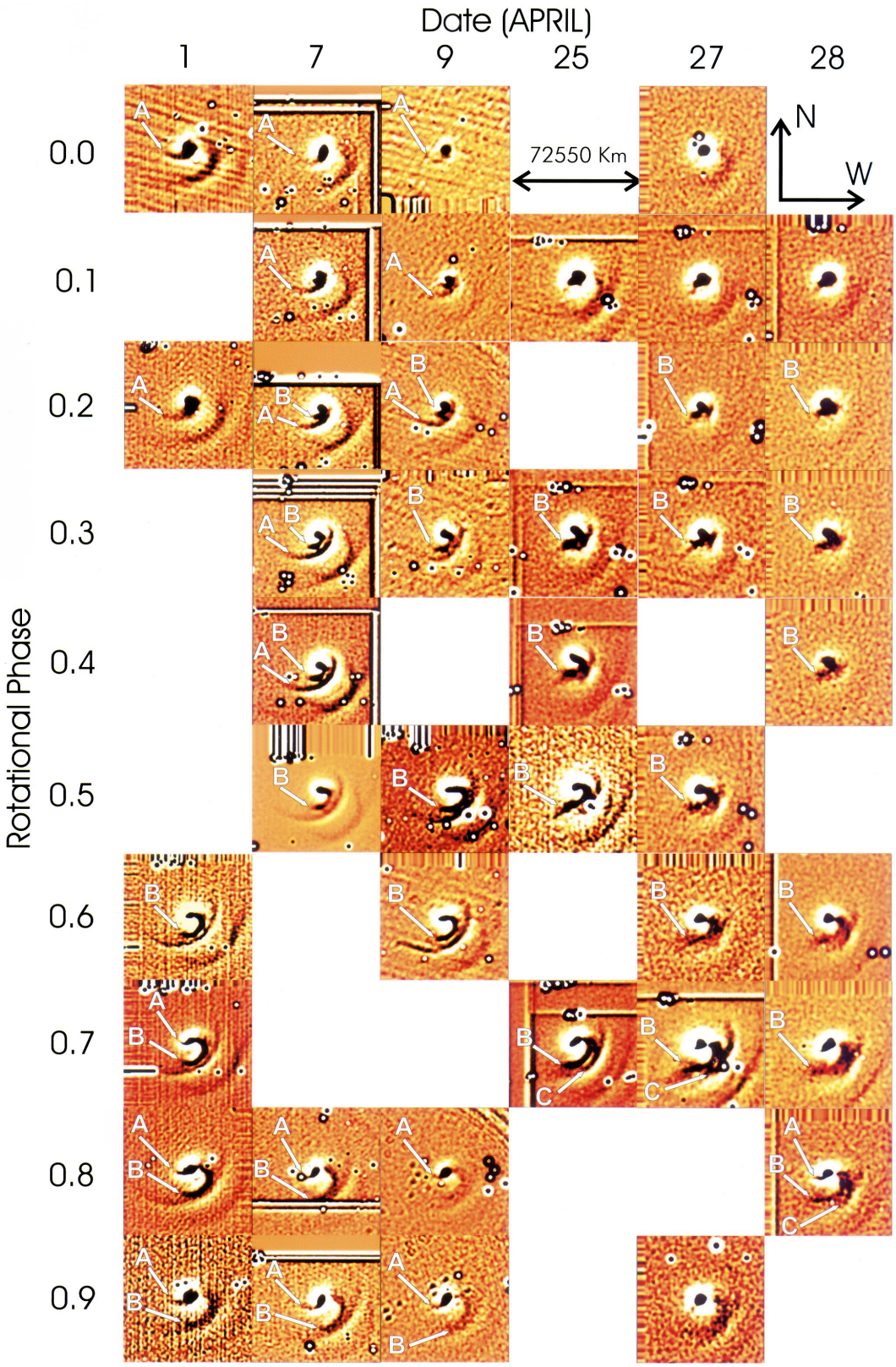

FIG. 1.—Processed images of the central coma of Hale-Bopp. The images are ordered day by day and phased according to the 11.35 hr period to show images of the same rotational phase in different days. The nuclear condensation is in the center of each image. Three spiral jets labeled A, B, and C and some expanding shells can be observed as dark curved structures.

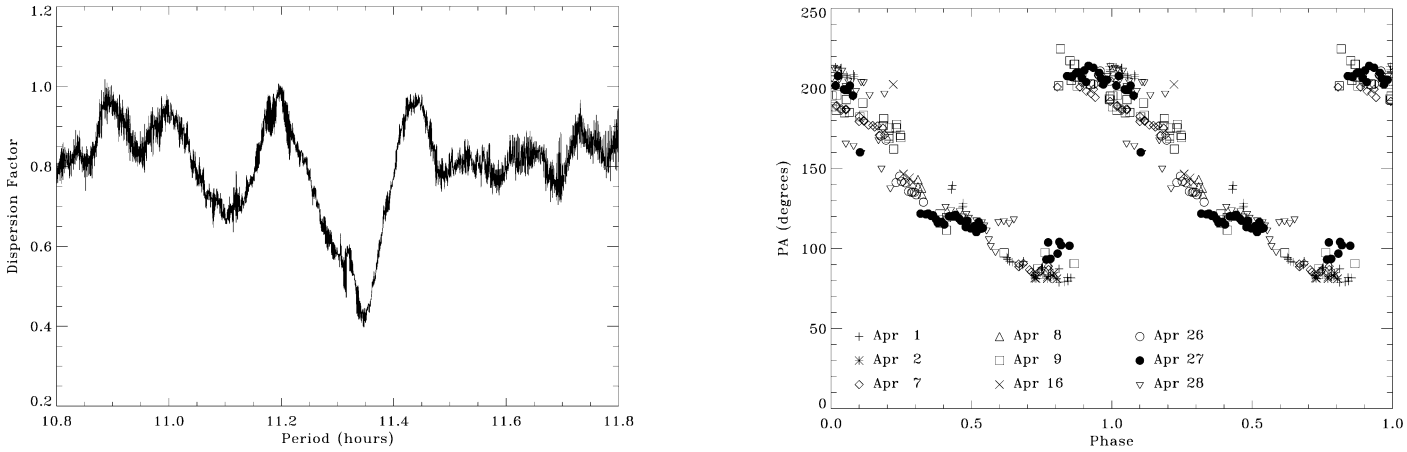

FIG. 2.—*Left:* Periodogram analysis by PDM (Stellingwerf 1978) using the full data set between 1997 April 1 and April 28. Note the clear minimum at 11.35 hr. *Right:* P.A. of the maximum intensity in the coma region between 5100 and 12,500 km from the nucleus (see text), phased according to the adopted period of 11.34 hr.

of equal rotational phase from different days. The rotation period of 11.35 ± 0.05 hr is the one for which images at the same rotational phase look more similar. The position angles of jets A and B (measured at their starting point close to the nucleus), their curvature, and the distance of the shells from the optocenter were taken into account to decide on the similarity of the images. The long series of observations, spanning an interval of about 1 month, has allowed us to determine very precisely the rotation period. The uncertainty of 0.05 hr represents the range of period values for which differences in images of equal rotational phase are not obvious between the beginning and end of April. This method is closely related to the identification of the jets, which is generally difficult because their appearance may dramatically change with time. However, this does not happen in our case. As seen in Figure 1, only small morphological variations in the structures were observed during 1997 April.

As a second and more quantitative method to assess the reliability of the derived period, we searched for a measurable feature in the images that repeats each rotation period and that is independent on the identification of the jets. More specifically, we have looked for periodic variations of the position angle (P.A.) of the dust coma's maximum intensity measured in a fixed ring around the nucleus. To this aim we took azimuthal profiles, using the unfiltered images, at different radial distances from the cometary optocenter, ranging from 5100 to 12,500 km. The limits of this ring are not crucial to compute the rotation period as far as the same structures repeat periodically in the coma. This way, the P.A. of the maximum intensity will change with the same periodicity for any ring we adopt. The particular limits used in this analysis are optimum in that closer to the nucleus the number of pixels entering the computation of the azimuthal profiles is too small and that farther than 12,500 km the jets are too faint. The profiles were rescaled to the same intensity level and then averaged to produce a single profile, whose maximum P.A. was determined by means of a Gaussian fit. This process gives the temporal evolution of the P.A. of the maximum intensity in the region described above. If the same jets repeat each rotation of the nucleus, this P.A. will also be the same. The resulting P.A.'s were employed to search for the most likely rotation period using the phase dispersion minimization (PDM) method (Stellingwerf 1978). The periodogram and phase curve are presented in Figure 2. The computed value of the rotation period is 11.34 ± 0.02 hr, which is in good agreement with that resulting from the application of the more qualitative method described above but with higher precision. The best rotation period value and the error are obtained using the parabolic form of the statistic (dispersion factor in Fig. 2) around its minimum. The quoted 68% (1 σ) confidence level corresponds to the interval obtained by increasing the minimum value of the statistic by unity (see Lampton, Margon, & Bowyer 1976, and references therein). This confidence level and the error obtained from the parabolic fit of the minimum are quadratically added in order to compute the uncertainty of the rotation period.

Usually, the azimuthal profiles have two maxima produced by jets A and B, of which we use the most intense maximum. The resulting phase curve (Fig. 2) shows that the rotation of the maximum has two discontinuities: one at phase 0.8 and a smaller one at phase 0.2. These discontinuities occur because the relative intensity of the two maxima observed in the profile changes during the rotation, giving an inflexion where the brightest maximum varies from being due to one jet to the other.

In addition, we have searched for possible variations of the rotation period due to precession effects, as suggested by Jorda et al. (1997). We applied the second method to two restricted data sets: images from April 7 to 9 and from April 25 to 28. The period obtained from the first data set is 11.35 ± 0.08 hr, while that obtained from the second is 11.4 ± 0.3 hr. In all cases, the significance of the rotation period computed as in Stellingwerf (1978) is well below 0.01 (a likelihood better than 99%).

5. DISCUSSION

As seen in Figure 1, the behavior of the jets was very stable during the month of observations, with only small morphological differences between the beginning and the end of April caused more likely by variations of the comet aspect angle. This supports the idea of a very stable jet production mechanism by active areas on the cometary nucleus if the same areas were active and always exposed to solar radiation during 1997 April. This morphological stability could represent a good test for the validity of the alternative hydrodynamic models proposed by Crifo & Rodionov (1996). The stable morphological

behavior, and the fact that the identification of the jets is unambiguous, has allowed us to obtain a very accurate rotation period for the nucleus of 11.34 ± 0.02 hr.

The stability of the jets contradicts the possible existence of a very complex rotation of the nucleus. However, Kidger et al. (1998) determined a periodicity of 20 ± 4 days in the apparition of the curved jets observed during 1995 and related this to the precession period. Any precession of the spin axis would introduce variations on the rotation period, as pointed out by Jorda et al. (1997). We have searched for such variations, but the rotation periods derived from the two restricted data sets are in good agreement. In any case, the small error obtained using the complete data set is an indication that we should not expect variations in the rotation period larger than 0.04 hr. It is important to stress, however, that the time sampling of our best observations, separated by an interval of ~20 days (similar to the suggested precession period), prevents us from ascertaining whether variations of the rotation period due to precession exist. The good agreement of our results with the 11.35 hr rotation period reported by Jorda et al. (1998) and with the 11.3 hr reported by Sarmecanic et al. (1997) at different epochs between February and late April suggests that any variation in the rotation period must be small.

The large size of Hale-Bopp's nucleus is probably the reason that the rotation is not particularly complex, since the time scale necessary for the nongravitational torque to modify the rotational state is proportional to r_n^2 (Jewitt 1992), where r_n is the equivalent radius of the nucleus.

6. CONCLUSIONS

Three spiral jet structures were observed in the near-infrared in comet Hale-Bopp's coma for several, almost complete, rotations between 1997 April 1 and April 28. As the appearance of the coma is identical in images obtained with the three narrowband filters used, we conclude that these structures are mainly dust jets.

A rotation period of the nucleus of 11.35 ± 0.05 hr was determined by comparing the jets in images obtained in different nights at equal rotational phases. We have used a new method to search for periodicities in the position angle of the dust coma's maximum intensity in a ring around the nucleus, using the PDM method (Stellingwerf 1978). The best rotation period value obtained is 11.34 ± 0.02 hr.

No variations of the rotation period with time due to precessional effects were found in our data. However, the time sampling of the observations, which is similar to the suggested spin precession period, does not allow us to discriminate the existence of such variations. We note, though, that the good agreement of our results with the rotation periods reported by other groups at different epochs lends support to the idea that, if they exist, these variations must be small. This would imply that Hale-Bopp's nucleus is close to its lowest rotation energy state.

The Carlos Sánchez Telescope in Teide Observatory is operated by the Instituto de Astrofísica de Canarias. We thank the Telescope Manager, Jesús Jiménez, for generous telescope access. We also thank Peter Hammersley for his helpful comments on the acquisition and reduction process and Pierre Colomb for his help on the PDM method. This project has been supported by the European Commission through the Activity "Access to Large-Scale Facilities" within the program "Training and Mobility of Researchers," awarded to the Instituto de Astrofísica de Canarias to fund European astronomers' access to its Roque de Los Muchachos and Teide Observatories (European Northern Observatory) in the Canary Islands. J. L. acknowledges support from the Instituto de Cooperación Iberoamericano.

REFERENCES

Crifo, J., & Rodionov, A. 1996, BAAS, 28, 1086
Jewitt, D. 1992, in Observations and Physical Properties of Small Solar System Bodies, ed. A. Brahic, J.-C. Gehrard, & J. Surdej (Lèige: Univ. Lèige, Institut D'Astrophysique), 699
Jorda, L., Lecacheux, J., & Colas, F. 1997, IAU Circ. 6583
Jorda, L., Lecacheux, J., Colas, F., Colom, P., Frappa, E., & Rembor, K. 1998, Earth Moon Planets, in press
Kidger, M. R., Serra-Ricart, M., Bellot Rubio, L., & Casas, R. 1996, ApJ, 461, L119
Kidger, M. R., et al. 1998, AJ, submitted
Lampton, M., Margon, B., & Bowyers, S. 1976, ApJ, 208, 177
Licandro, J., et al. 1998, Earth Moon Planets, in press
Sarmecanic, J., Osip, D. J., Fomenkova, M., & Jones, B. 1997, IAU Circ. 6600
Sekanina, Z. 1981, AJ, 86, 1741
———. 1998, AJ, 494, L121
Stellingwerf, R. 1978, ApJ, 224, 953